Railway Sciences

575

Received 21 June 2024
Revised 2 July 2024
Accepted 3 July 2024

Estimation of speed-related car body acceleration limits with quantile regression

Jianli Cong
China Academy of Railway Sciences Corporation Limited, Infrastructure Inspection Research Institute, Beijing, China
Hang Zhang
School of Civil Engineering, Beijing Jiaotong University, Beijing, China and Planning and Standard Research Institute, National Railway Administration, Beijing, China
Zilong Wei, Fei Yang and Zaitian Ke
China Academy of Railway Sciences Corporation Limited, Infrastructure Inspection Research Institute, Beijing, China
Tao Lu, Rong Chen and Ping Wang
MOE Key Laboratory of High-Speed Railway Engineering, Southwest Jiaotong University, Chengdu, China, and
Zili Li
Department of Engineering Structures, Delft University of Technology, Delft, Netherlands

Abstract

Purpose – This study aimed to facilitate a rapid evaluation of track service status and vehicle ride comfort based on car body acceleration. Consequently, a low-cost, data-driven approach was proposed for analyzing speed-related acceleration limits in metro systems.

Design/methodology/approach – A portable sensing terminal was developed to realize easy and efficient detection of car body acceleration. Further, field measurements were performed on a 51.95-km metro line. Data from 272 metro sections were tested as a case study, and a quantile regression method was proposed to fit the control limits of the car body acceleration at different speeds using the measured data.

Findings – First, the frequency statistics of the measured data in the speed-acceleration dimension indicated that the car body acceleration was primarily concentrated within the constant speed stage, particularly at speeds of 15.4, 18.3, and 20.9 m/s. Second, resampling was performed according to the probability density distribution of car body acceleration for different speed domains to achieve data balance. Finally, combined with the traditional linear relationship between speed and acceleration, the statistical relationships between the speed and car body acceleration under different quantiles were determined. We concluded the lateral/vertical quantiles of 0.8989/0.9895, 0.9942/0.997, and 0.9998/0.993 as being excellent, good, and qualified control limits, respectively, for the lateral and vertical acceleration of the car body. In addition, regression lines for the speed-related acceleration limits at other quantiles (0.5, 0.75, 2s, and 3s) were obtained.

This study was funded by the National Natural Science Foundation of China (NSFC) under No. 52308473, the National Key R&D Program under No. 2022YFB2603301 as well as the China Postdoctoral Science Foundation funded project (Certificate Number: 2023M743895).

Railway Sciences
Vol. 3 No. 5, 2024
pp. 575-592
Emerald Publishing Limited
e-ISSN: 2755-0915
p-ISSN: 2755-0907
DOI 10.1108/RS-06-2024-0019

Originality/value – The proposed method is expected to serve as a reference for further studies on speed-related acceleration limits in rail transit systems.

Keywords Car body acceleration, Track status monitoring, Speed-related acceleration limit, Quantile regression, Vehicle ride quality

Paper type Research paper

1. Introduction

In rail transit, the accurate evaluation of track status is among the top priorities for safe railway operations. In general, the measured data from track geometry car (TGC) can be used directly for the evaluation of track status based on the track quality index (TQI), track irregularity spectrum, and peak values of measured track geometry (Haigermoser, Luber, Rauh, & Graefe, 2015; Xu & Zhai, 2017a, b; Lasisi & Attoh-Okine, 2018). Compared with the periodic inspection data from TGC, using the car body acceleration of commercial trains for estimating track service status is an effective and low-cost method (Hodge, O'Keefe, Weeks, & Moulds, 2015; Wei, Liu, & Jia, 2016; Lee, Choi, & Kim, 2012). The key lies in the determination of the limits for car body acceleration. However, this is plagued by the difference in acceleration limits caused by track alignment, track geometry, track structure, vehicle suspensions, speed, and other factors between different lines, particularly in metro systems (Haigermoser *et al.*, 2015; Mohammadi, He, Ghofrani, Pathak, & Aref, 2019). Thus, this study explored an efficient and economical method for determining the speed-related acceleration limits to formulate an adaptive acceleration limit for a specific track line.

The condition evolution of key structures in a vehicle–track system is a random process, and the random vibration response of the system follows the probability density evolution (Xu & Zhai, 2017a, b, 2018; Shan, Wang, Zhang, & Zhou, 2021; Shan, Li, & Zhou, 2023). A quantile regression approach can be used to determine the acceleration limit of the measured data according to probability statistics (Correia *et al.*, 2017; He, Zheng, & Xu, 2019). Consider track geometry as an example. It is the result of the random evolution of track status (Higgins & Liu, 2018; Audley & Andrews, 2013), including longitudinal irregularity, horizontal irregularity, cross-level, and twist, consequently forming a composite random irregularity with multiwavelength components. This results in different frequencies and amplitudes of car body acceleration at multiple speeds (Haigermoser *et al.*, 2015; Ahlin & Granlund, 2002; Kim, Kwon, Kim, Park, & Park, 2003). Therefore, the use of the same car body acceleration limit to diagnose the track status without considering the speed is inappropriate.

In the past, experienced workers examined the track status according to their personal feelings while riding a metro train. The detection results were dependent on their engineering experience, resulting in low accuracy (Hodge *et al.*, 2015). Currently, high-precision sensors are often installed on the car body to improve detection accuracy (Lederman *et al.*, 2017; Zoccali, Loprencipe, & Lupascu, 2018; Mori, Sato, Ohno, Tsunashima, & Saito, 2013). Based on the measured data of the vertical and lateral acceleration of the car body, half-peak limits of 0.12–0.15 and 0.1–0.12 g have been specified to judge whether the instantaneous acceleration of the car body exceeded the limit (Tsunashima & Hirose, 2020). A metro system has diverse track structures, small radius curves, and frequent acceleration or deceleration. Moreover, the instantaneous acceleration limits of the car body cannot be directly used to diagnose the track status in a metro system (Li, He, & Wang, 2022). Thus, the acceleration limits must be modified according to the measured data along with the incorporation of the influence of the vehicle speed.

The rapid increase in traffic volume, speed, and heavy maintenance workloads has motivated track departments to develop new methods for assessing existing infrastructure conditions and determining where upgrades are required. Li *et al.* (2022) proposed an extended auto-encoder to estimate track longitudinal irregularity through car body acceleration, which significantly improved the measurement efficiency of track irregularity. Tsunashima, Naganuma, and Kobayashi (2014) proposed that the estimation of track irregularities from car body acceleration is an inverse problem. Consequently, they designed a Kalman filter according to car body motions to solve this problem. Kulkarni, Qazizadeh, Berg, Carlsson, and Stichel (2022) developed a vehicle-running instability detection algorithm to reveal the coherence between lateral and longitudinal accelerations during vehicle hunting. Certain international standards have compared the filtered lateral acceleration with a certain limit criterion for detecting vehicle hunting (technical specification for interoperability; UIC 515–1, n.d.). Abdulrazagh, Hendry, Gül, Roghani, and Toma (2022) applied car body-weighted acceleration to evaluate ride quality and track roughness. Sun, Chi, Cai, Gao, and Liang (2021) proposed an original method to exploit peak value information for evaluating car body hunting instability. Consequently, they compared it with the Sperling, mean comfort standard, and continuous comfort methods. The above studies demonstrated that evaluating the track status based on car body acceleration is an economical, efficient, and accurate measurement method. Moreover, this technology has been widely used in actual rail transit operations. However, these studies did not consider speed in the acceleration limits.

Considering all the existing limitations, this study developed an innovative method to determine acceleration limits based on quantile regression. Independently developed sensing terminals were used to obtained high-quality and high-precision car body accelerations. Further, a data fusion method was adopted to evaluate the vehicle speed and position. Furthermore, the quantile regression method was used to explore the statistical relationship between the vehicle speed and car body acceleration. This method is robust and comprehensively considers the effect of multifactor coupling on the car body acceleration. Thus, this study can supplement or modify the car body acceleration control limits obtained using the existing linear regression method.

The contributions of this paper are summarized as follows:

(1) A data balancing method was proposed to eliminate the data imbalance caused by different train operation durations at different speeds.

(2) A quantile regression optimization model was proposed to fit the nonlinear relationship between speed and car body acceleration under multiple factors. Moreover, speed-related acceleration limits for different evaluation levels of track status (excellent, good, and qualified) were obtained.

The remainder of this paper is organized as follows. Section 2 describes the methodology of the data analysis, including data acquisition and preprocessing, data balancing, and quantile regression. Section 3 introduces the field test for measuring the car body acceleration in the metro line and reveals the joint probability distribution of the speed and car body acceleration. In Section 4, the evaluation of the track status based on the relationship between speed and car body acceleration is compared using traditional formulas and quantile regression. Finally, conclusions are presented in Section 5.

2. Methodology

2.1 Data acquisition and preprocessing

This study developed a low-cost sensing terminal that can be installed on a train. It is a noninvasive acceleration measurement device that does not require power from the operating trains. It had a built-in acceleration sensor with a sampling frequency of 200 Hz and a lithium battery. For the round trip of a metro train, the sensing terminal measurement time could be flexibly set according to the train timetable, and the car body acceleration in a single round trip was recordable.

Before using the measured data to investigate and determine the speed-related acceleration limits, the data must be preprocessed to ensure reliability. This includes the following three main parts:

(1) Coordinate system transformation: A method was proposed to transform the measured accelerations from the coordinate system of the sensing terminal to that of the metro train. This included the transformations in the vertical, longitudinal, and lateral directions. Using this method, the placement direction of the sensing terminal need not be adjusted or fixed to a specific position during the measurement process. This rendered the measurement of the sensing terminal more convenient. The relevant algorithms can be found in Wang, Cong, Wang, Liu, and Tang (2019).

(2) Verification of the acceleration sensor accuracy: After coordinating the system transformation, we verified the measurement accuracy of the low-cost sensor terminal and compared it with that of the high-precision sensor. In the field test, the measured data of the two types of sensors were consistent with traditional evaluation indexes. These included the standard deviation, Sperling index, and ISO-2631 weighted acceleration index, as described by Cong, Gao, Wang, Chen, and Wang (2020).

(3) Speed and position estimation of metro trains in GPS-free environments: A interface was not required to obtain the speed and position information from an in-service train. The initial estimations of this information were obtained via the integration and double integration of longitudinal accelerations. The waveform correlation coefficient of the sensor terminal-measured data between different vehicles of the train was relatively high; however, a time delay was observed. Further, the initial estimation errors of speed and position were modifiable based on the data fusion model. Moreover, the field test showed that the maximum position error could be controlled within 20 m. The relevant algorithm can be found in Wang *et al.* (2019).

2.2 Data balancing

Owing to the operation mode of metro trains, the duration of train operation varies at different speeds, which results in a data imbalance of the car body acceleration corresponding to the speed. In addition, there is a significant difference in the distribution of car body acceleration in the speed dimension. This distribution directly affects the regression relationship between the speed and car body acceleration, which is a biased estimation. Therefore, we proposed a data-balancing method that performed distribution statistics on car body acceleration at different speeds. Consequently, the car body acceleration was resampled at different speeds according to the same distribution characteristics to achieve data balancing; thus, the number of car body accelerations at different speeds was consistent. The specific steps are as follows.

After adjusting the train speed and position in a GPS-free environment, the dataset of car body acceleration in the train speed dimension is represented as $\{(v_i, a_i), i = 1, 2, \cdots, N\}$, a moving window with a length of 1 m/s moves in the speed dimension, and the overlapping length of the moving windows is 0.5 m/s. The number of moving windows is calculated as follows:

$$n = \frac{v_{max} - v_{min} - 1}{0.5} \tag{1}$$

where v_{max} and v_{min} denote the maximum and minimum speeds in the dataset (m/s), respectively.

The distribution of car body acceleration under different moving windows was estimated, and the distribution parameter varied with an increase in train speed, as shown in Figure 1. The Kullback–Leibler (KL) divergence was used to measure the degree of matching between two probability distributions, as shown in Eq. (2).

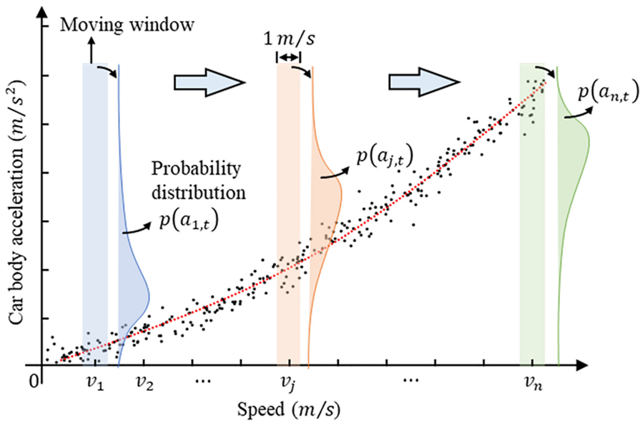

Source(s): Authors' own work

Figure 1.
Estimation of car body acceleration distribution using different moving windows

$$D_{KL}(p\|f) = \sum_{t=1}^{q} p(a_{j,t}) log\left(\frac{p(a_{j,t})}{f(a_{j,t})}\right), j = 1, 2, \cdots, n \tag{2}$$

where $p(\bullet)$ is the true distribution of car body acceleration under the j-th moving window, $f(\bullet)$ is the target distribution, $a_{j,t}$ is the t-th data point of the j-th moving window, and q is the total number of data points in the j-th moving window. If the two distributions match perfectly, the following equation is satisfied:

$$D_{KL}(p\|f) = 0 \tag{3}$$

The car body acceleration is the random response of the vehicle-track coupling system, and a logarithmic normal distribution was used to approximate the true probability distribution $p(a_{j,t})$ at different speeds. The model parameters of the target distribution $f(a_{j,t})$ are calculated as follows:

$$\begin{cases} m_j = \dfrac{\sum_{t=1}^{q} a_{j,t}}{q} \\ \delta_j = \sqrt{\dfrac{\sum_{t=1}^{q} (a_{j,t} - m_j)}{q-1}} \\ \mu_j = log\left(m_j^2 \Big/ \sqrt{\delta_j + m_j^2}\right) \\ \sigma_j = \sqrt{log(\delta_j / m_j^2 + 1)} \\ f(a_{j,t}, \mu_j, \sigma_j) = \dfrac{1}{a_{j,t}\sqrt{2\pi}\sigma_j} exp\left[-\dfrac{1}{2\sigma_j^2}(ln\, a_j - \mu_j)^2\right] \end{cases} \tag{4}$$

where m_j, δ_j is the mean and standard deviation of the j-th moving window of the car body acceleration, respectively. μ_j and σ_j are the mean and standard deviation parameters of the logarithmic normal distribution under the j-th moving window of the car body acceleration, respectively, and $f(\cdot)$ is the logarithmic normal distribution formula for the j-th moving window of the car body acceleration.

According to equation (4), the logarithmic normal distribution of the car body acceleration was resampled, and the process is as follows:

$$\begin{cases} r_j \sim N(0, \delta_j) \\ a_j' = \mu_j + \sigma_j \cdot log(r_j) \end{cases} \tag{5}$$

where r_j is the random data of the j-th moving window, following a normal distribution with a mean of 0 and a standard deviation of δ_j. Further, a_j' is the resampling result of the car body acceleration under j-th moving, which satisfies the distribution $f(a_{j,t}, \mu_j, \sigma_j)$.

Based on the above data preprocessing, research on speed-related acceleration limits in this study can be conducted.

2.3 Quantile regression

In rail transit, the evaluation threshold of the car body acceleration is related to whether it truly reflects the track condition. Moreover, the acceleration limits should not be the same at different speeds. According to GBT 5599–1985 "Railway vehicles-specification for evaluation the dynamic performance and accreditation test," the vehicle running stability is evaluated according to the average maximum vibration acceleration of the car body. When the operating speed V is < 140 km/h, the average maximum vibration acceleration of the car body should satisfy the stability requirement, as follows:

$$\overline{A}_{max} \leq 0.00027V + C \tag{6}$$

where $\overline{A}_{max}$ is the average maximum vibration acceleration of the car body (g), V is the train speed (km/h), and C is a constant (Table 1).

It is the most direct and economical method for diagnosing track status and vehicle riding comfort based on the vertical and lateral accelerations of the car body. However, there exist certain differences between metro systems and ordinary railways, and it is unreasonable to directly apply the aforementioned average maximum acceleration of a car body to a metro system. Similarly, the correlation between the car body acceleration and speed in a metro system can be defined as follows:

$$\widehat{A} = \beta_0 + \beta_1 v \tag{7}$$

where $\widehat{A}$ is the predicted value of car body acceleration, v is the vehicle running speed (m/s), and β_0 and β_1 are the parameters to be determined for the regression model.

Table 1.
C values

	C	
Running stability level	Vertical vibration	Lateral vibration
Excellent	0.025	0.010
Good	0.030	0.018
Qualified	0.035	0.025

Source(s): Authors' own work

Linear regression aims to fit a straight line based on the measured data and predict the acceleration limit $\widehat{A}$ based on the vehicle speed V. To estimate the slope regression parameters that determine such a line, the least-squares method is commonly used. Given a dataset of observations $\{v_i, a_i\}(i = 1, 2, \cdots, n)$, the parameters ($\beta_0$, β_1) can be estimated based on the following least-squares estimate (LSE) model:

$$arg \min_{a} \frac{1}{2}\|a_i - \beta_0 - \beta_1 v_i\|^2 \tag{8}$$

where a_i and v_i are the acceleration and speed of the vehicle, respectively, at point i.

Quantile regression provides more information than the traditional conditional average models. It can be used to analyze univariate functional relationships under multi-factor uncertain conditions (Yu, Lu, & Stander, 2003). Moreover, it can be used to analyze different quantile values of car body acceleration corresponding to vehicle speeds and formulate multilevel acceleration limits.

The parameter vector is usually estimated through the quadratic loss function $\widehat{Q}_a(\tau)$.

$$\begin{cases} \widehat{Q}_a(\tau) = argmin_{\widehat{A}_{\tau i} \in R}\left(\sum_{i:a_i \geq \widehat{A}_{\tau i}} \tau\left|a_i - \widehat{A}_{\tau i}\right| + \sum_{i:a_i < \widehat{A}_{\tau i}} (1-\tau)\left|a_i - \widehat{A}_{\tau i}\right|\right) \widehat{A}_{\tau i} = \beta_{0,\tau} + \beta_{1,\tau} V_i \end{cases} \tag{9}$$

where $\widehat{Q}_a(\tau)$ is the error between the measured data and fitting function under the τ quantile, $\widehat{A}_{\tau i}$ is the fitting result under the τ quantile, $\beta_{0,\tau}$ and $\beta_{1,\tau}$ are the fitting parameters under the τ quantile, and V_i is the vehicle speed at point i.

Owing to the metro train operation model, the train duration varies at different speeds, resulting in imbalanced car body acceleration data at different speeds. First, the acceleration distribution of the car body under different speed ranges was obtained and calculated by increasing the speed interval by 1 m/s, the overlapping window length was 0.5 m/s. Subsequently, resampling was performed to achieve data balance according to the distribution of the car body acceleration. Finally, quantile regression was performed for the balanced data of the car body acceleration and speed.

Vehicle vibration is attributable to wheel-rail contact interaction under the excitation of track irregularities. Simultaneously, it is affected by other factors including small radius curves, speed, and vehicle suspension. Therefore, a more reasonable approach involves using quantile regression to process a significant amount of measurement data and determine the multilevel acceleration limits. This would provide a reference for vehicle shaking and ride comfort assessment.

3. Experimental setup and data description

3.1 Field test

Car body acceleration is the result of vehicle–track interactions in complex environments, including track alignment, track geometry, track structure, speed, and other factors. However, the control limit value of car body acceleration cannot be determined using a simulation model. Internet of Things (IoT) sensing technology can be used to collect car body acceleration data, as shown in Figure 2(a), and speed-related acceleration limits can be formulated based on the analysis of massive measured data.

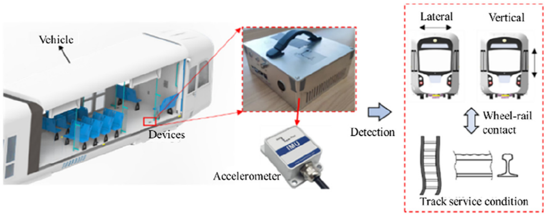

Schematic of the condition monitoring of the vehicle-track system by sensing terminal

(a)

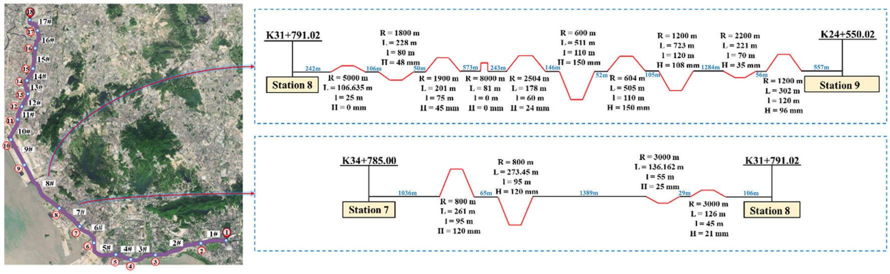

Diagram of metro line to be measured and plane alignment of station intervals #7 and #8

(b)

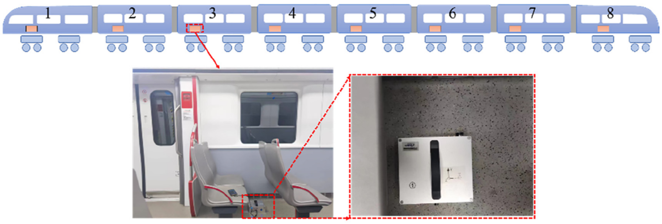

Metro train formation and placing onboard sensing terminals

(c)

Figure 2.
Field test set-up

Source(s): Authors' own work

The field tests were conducted on a Chinese metro train operating at a speed of 120 km/h. The total length of the metro line was 51.95 km, with 18 stations and various radius curves, as shown in Figure 2(b). An onboard sensing terminal was used to continuously record the accelerations at a specified sampling frequency. The field test parameters are listed in Table 2. The layout and location of the sensing terminals are illustrated in Figure 2(c). Eight sensing terminals were placed on the floors of different vehicles on the train. This experiment required 2.5 h to measure the car body acceleration in a single round trip of the train, and the measured data in $8 \times 17 \times 2 = 272$ metro operation sections were used to determine the speed-related acceleration limits. Notably, the placement distance between the adjacent sending terminals was recorded, combined with the delay of car body acceleration data from adjacent terminals, to correct the speed and position of metro trains.

3.2 Dataset description

The running speeds of the metro vehicles within each section were obtained after the data fusion of multiple onboard sensing terminal test data. In operation Sections #7 and #8, the durations with approximately constant vehicle speeds in the range of 15–25 m/s were approximately 100 and 296 s (accounting for 56% and 80% of the total time in the sections, respectively), as shown in Figure 3(a). This is a common operation mode in metro systems, and the vehicle speed profile is the same for each run. It results in an unbalanced proportion of car body acceleration data for different speed ranges.

Figure 3(b) shows the car body lateral and vertical accelerations measured by the terminal in Section #8. The track plane alignment in this operation section is shown in Figure 2(b), particularly in the curved section. Here, the unbalanced superelevation produced a large centrifugal force on the vehicle, and the maximum lateral acceleration of the car body exceeded 0.4 m/s^2, as shown in Figure 3(b).

In addition to the vehicle speed, the car body acceleration was affected by several factors. The median, upper, and lower quartile values of the lateral and vertical accelerations of the trains in the 17 station sections were significantly different, as shown in Figure 3(c). The red dots exceeding the upper quartile value (75%) exhibited a data mining value and could not be eliminated as outliers in the data statistics, thereby reflecting the service status of the track. The differences in the car body lateral and vertical accelerations in the 17 operation sections reflected the differences in track status, including track alignment and geometry. Consequently, the track service status of each section was compared and evaluated. However, the measured train repeatedly operated on the same line, and the speed profile was the same for each run. Nevertheless, the track status continued to evolve under millions of wheelset passages. Therefore, the speed-related acceleration limits must be determined to evaluate track conditions.

In general, the speed profile of metro trains in automatic train operation (ATO) mode is not affected by the operation level of the driver. Figure 4 shows the frequency statistics of the measured data of the eight sensing terminals in the speed-acceleration dimension. Under the speed dimension, the train speed was concentrated at 15.4, 18.3, and 20.9 m/s, which were determined by the ATO mode. Owing to the differences in the track status along the metro line, the car body acceleration was distributed within a certain range at the same speed, and the acceleration amplitude increased slightly with increasing speed. In the acceleration dimension, the statistical distributions of the lateral and vertical acceleration obeyed lognormal distributions, which were $lnN(-2.78, 0.67^2)$ and $lnN(-2.21, 0.38^2)$, respectively. As evident, the vertical acceleration distribution was more concentrated, and the lateral excitation of the metro line was more significant.

Figure 5 shows the probability density distribution of the lateral and vertical accelerations of the car body at different operating speeds, including 0–10, 10–15, 15–20, 20–25, 25–30, and

Item	Parameter	Value or description
Sensing terminal	Sensor type	Accelerometer
	Maximum range	2*g*
	Sampling frequency	200 Hz
	RAM	2 GB
Metro line	Whole line length	51.95 km
	Number of stations	18
	Train formation	A-type train with 8-car

Source(s): Authors' own work

Table 2. Parameters of the field test

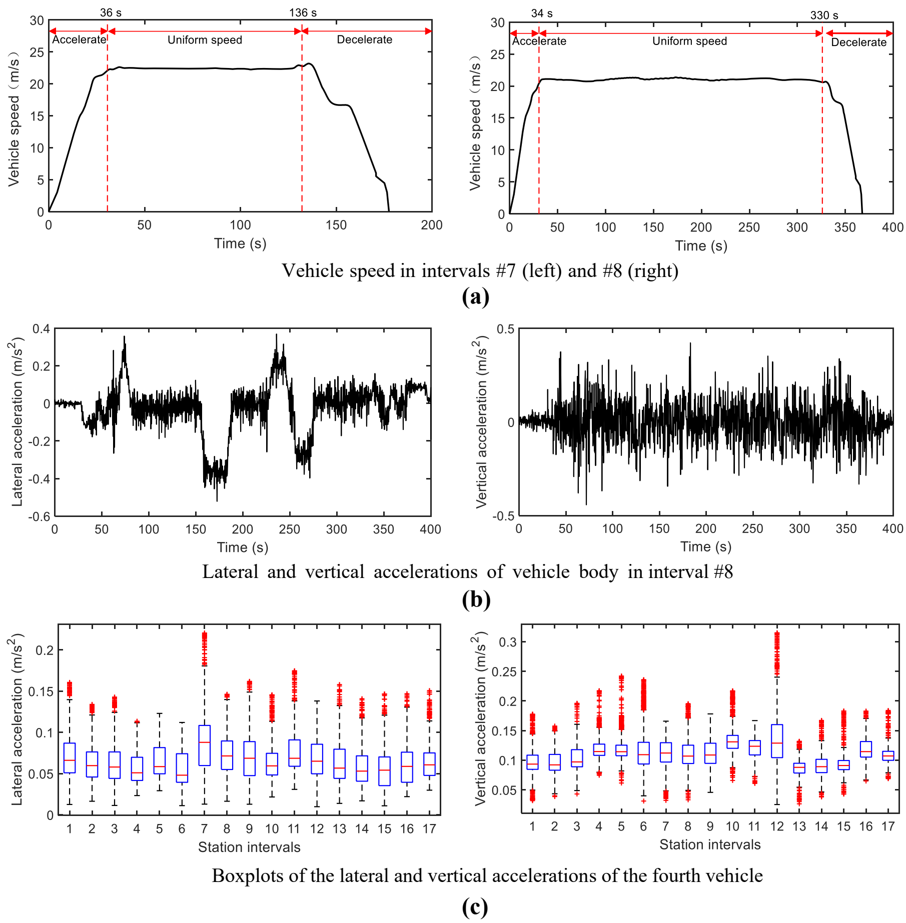

Figure 3.
Measured data for the on-board sensing terminals: (a) the train speed profile in metro sections #7 and #8; (b) lateral and vertical

Source(s): Authors' own work

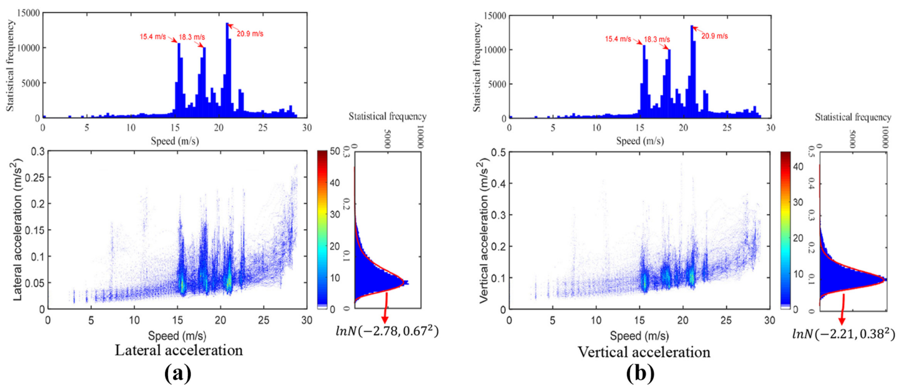

Figure 4.
Statistical distribution of measured data in speed-acceleration dimension

Source(s): Authors' own work

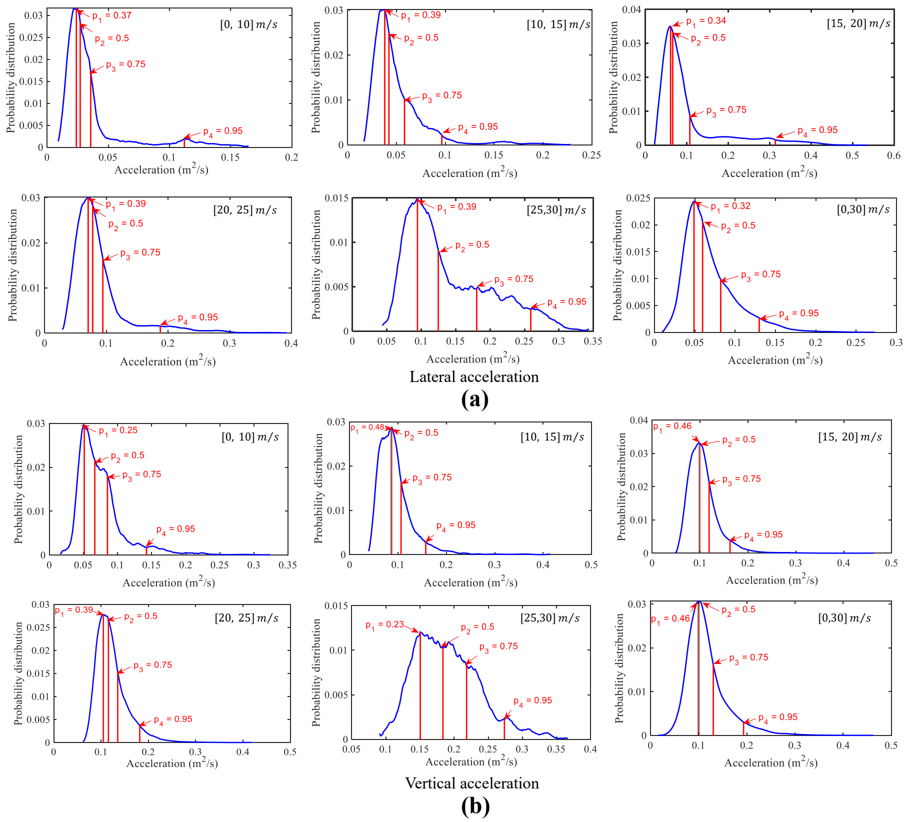

Figure 5. Probability distribution of car body acceleration in different speed ranges

Source(s): Authors' own work

0–30 m/s. There was a long tail effect in the probability density distribution. The cumulative probability density corresponding to the peak value was within 0.2–0.5. Moreover, a difference was observed between the lateral and vertical accelerations of the car body corresponding to the same specific quantile (e.g., 0.5, 0.75, and 0.95) in the multispeed range. This probability density distribution reflected the random vibration process of the vehicle–track system, and the track status was evaluated by considering the speed-related acceleration amplitude under different quantiles.

4. Results

4.1 Conventional assessment of speed-related acceleration for track status monitoring

As the car body acceleration exceeded the control limits owing to being a small probability event, the τ value was significantly different from the traditional quantiles, such as the median (50%) and quartile (75%). Using Equation (6), that the slope of the relationship between the vehicle speed and the average maximum vibration acceleration was obtained as 0.00027 at different running stability levels, as indicated by the dashed line in Figure 6. The quantiles corresponding to different running stability levels were standardized as τ for quantile regression, as shown in Table 3. The fitting function parameters corresponding to τ were obtained according to the loss function of Equation (9), and the fit index R_τ^2 is listed in Table 4.

Figure 6 shows the quantile regression lines of the lateral and vertical acceleration with τ fitted by LSE (solid line). Moreover, according to GBT 5599–1985, the average maximum vibration acceleration of the vehicle body was obtained (dashed line). The three dashed lines corresponded to the excellent, good, and qualified track statuses. The slopes of the dashed lines were the same; however, the intercepts were different. First, the lateral acceleration indicated that the 0.8989 quantile regression fitted line and excellent limit line intersected at a speed of 19 m/s. Whereas, the 0.9942 quantile regression fitted line and good limit line intersected at a speed of 20 m/s. The qualified line corresponded to almost all the values above the 0.9998 quantile regression fitted line. It can be concluded that the lateral acceleration within the 272 metro sections was at a good level. However, the slope of the existing control limit line was less than that of the quantile regression line. The existing control limits were higher when the vehicle speed was low and lower when the vehicle speed was high. Furthermore, the fitted line of the quantile regression was consistent with the

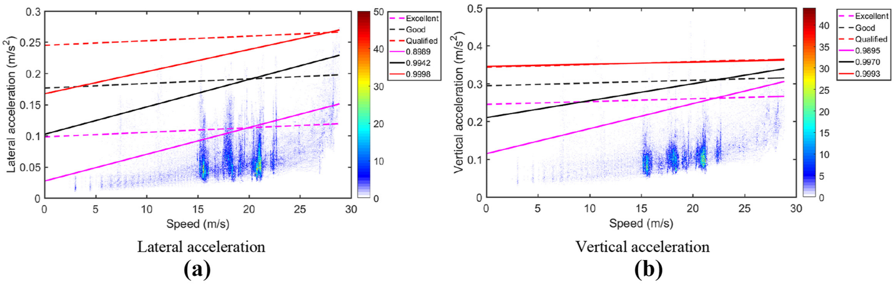

Source(s): Authors' own work

Figure 6. Quantile regression lines corresponding to different τ values fitted by LSE (solid line), and the average maximum vibration acceleration of the car body as shown with the dashed line

Table 3. Quantile corresponding to the conventional assessment method

Fitting function	Direction	Running stability level	C	τ
$\overline{A}_{max} = 0.00027V + C$	Lateral	Excellent	0.010	0.8989
		Good	0.018	0.9942
		Qualified	0.025	0.9998
	Vertical	Excellent	0.025	0.9895
		Good	0.030	0.9970
		Qualified	0.035	0.9993

Source(s): Authors' own work

Table 4. Coefficient of fitting function and its fit index R_τ^2

Fitting function $A_\tau = \beta_1 V + \beta_0$	τ	Polynomial coefficient β_0	β_1	R_τ^2
Lateral	0.8989	0.0272	0.0043	0.9380
	0.9942	0.1022	0.0044	0.9850
	0.9998	0.1673	0.0035	0.9990
Vertical	0.9895	0.1148	0.0066	0.9862
	0.9970	0.2099	0.0045	0.9929
	0.9993	0.3453	5.696e−4	0.9972

Source(s): Authors' own work

overall change trend of the car body acceleration, and the vertical acceleration was mostly at an excellent level relative to the lateral acceleration.

Therefore, directly evaluating the car body acceleration of the metro train using the conventional control limits is considered inappropriate. The quantile regressions at different τ values can better evaluate the lateral and vertical acceleration of the metro train. Here, the quantile regression lines of the lateral and vertical τ values 0.8989 and 0.9895, 0.9942 and 0.9970, and 0.9942 and 0.9970 were recommended as the excellent, good, and qualified control limits corresponding to car body lateral and vertical acceleration, respectively.

4.2 Speed-related acceleration limits in different quantiles after data balancing

Notably, the car body acceleration was relatively concentrated at a speed of 15–21 m/s. Naturally, the car body acceleration in this speed range accounted for a large proportion, which resulted in biased statistics for the car body acceleration in other speed domains, as shown in Figure 7(a) and 7(b). This natural imbalance in the car body acceleration resulted in a statistical deviation. Resampling can be performed according to the lognormal distribution of the car body acceleration at different speed ranges to achieve data balance. Figure 7(c) and 7(d) show the statistical distribution characteristics of the car body acceleration and speed after data balancing.

Figure 8 shows the car body acceleration distribution at different speeds after data balancing. The results were different from those in Figures 4 and 6, particularly when at speeds of 15, 18, and 21 m/s. The data distribution at each speed was balanced. However, the balanced car body acceleration distribution still conformed to the lognormal distribution, and the distribution parameters exhibited no evident changes.

To facilitate the track maintenance department in analyzing the measured data, the adoption of speed-related acceleration limits under different quantiles is recommended, as shown in Figure 9. The quantile adopted is consistent with that in Figure 6. The speed-related acceleration limits within different quantiles are listed in Table 5 and can be used as the basis for the metro system to evaluate the track status.

According to the probability distribution (Figure 5) of car body acceleration, the probability density values corresponding to 0.5, 0.75, 2σ, and 3σ, respectively, were selected

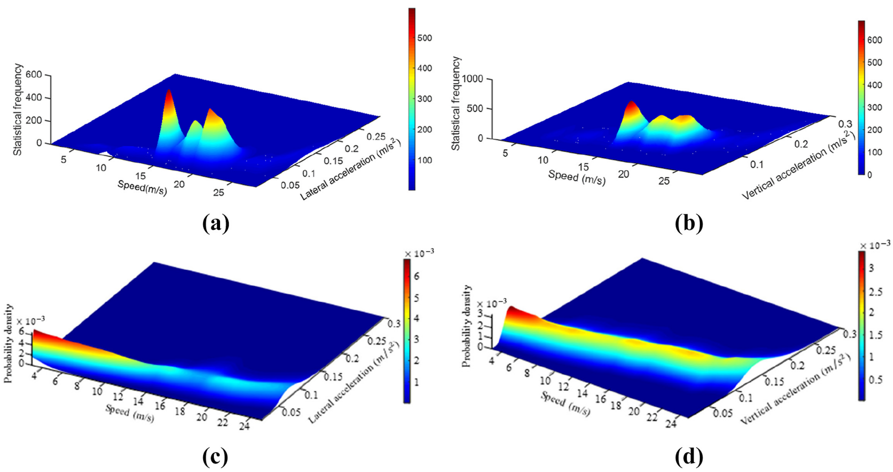

Source(s): Authors' own work

Figure 7. Probability distribution of speed-related acceleration: (a), (b) before data balancing; (c), (d) after data balancing

as the regression quantiles, as shown in Figure 10. The linear function parameters corresponding to the different quantiles are listed in Table 6. As evident, 95% of the car body accelerations were distributed below the 2σ quantile divider at different speeds.

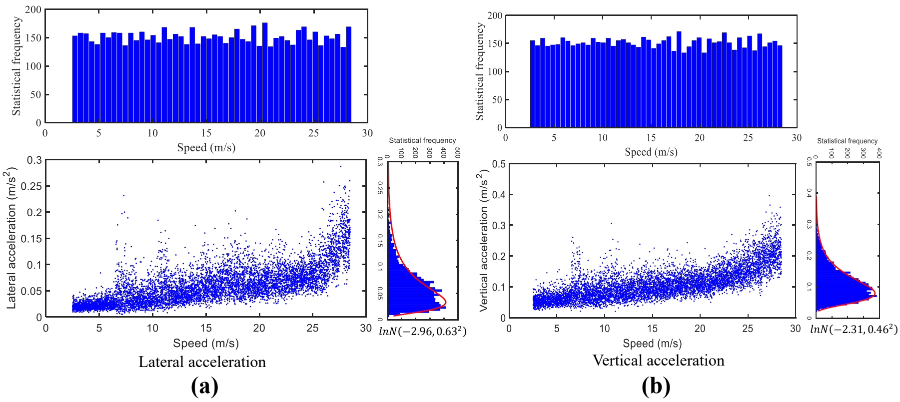

Source(s): Authors' own work

Figure 8.
Lateral and vertical acceleration of the vehicle body after data balancing, and data distribution characteristics of the vehicle speed and acceleration

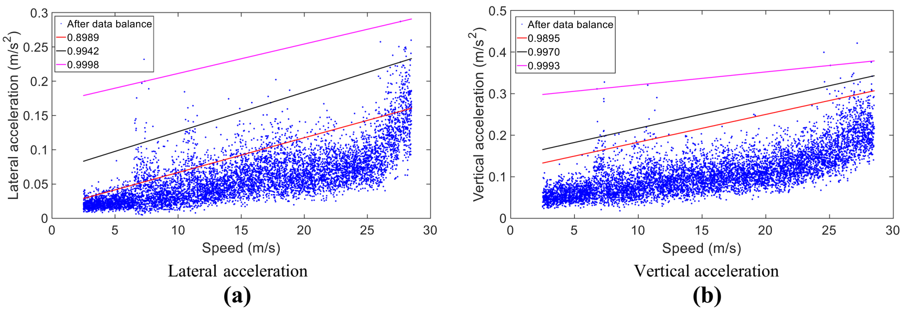

Source(s): Authors' own work

Figure 9.
Quantile regression lines of excellent, good, and qualified control level in different τ values for balanced data

Table 5.
Fitting parameters corresponding to the excellent, good, and qualified control levels of car body lateral and vertical acceleration

Vibration direction	τ	Function parameters β_0	Function parameters β_1	Control level
Lateral	0.8989	0.0163	0.0051	Excellent
	0.9942	0.0689	0.0058	Good
	0.9998	0.0015	0.0315	Qualified
Vertical	0.9895	0.0621	0.0066	Excellent
	0.9970	0.1484	0.0068	Good
	0.9993	0.2902	0.0031	Qualified

Source(s): Authors' own work

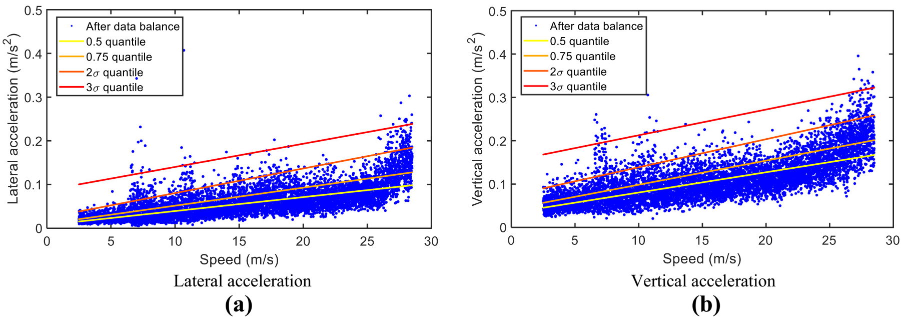

Source(s): Authors' own work

Figure 10. Quantile regression lines in other τ values for balanced data

Vibration direction	Regression function	Vibration direction	Regression function
Lateral	$A_{0.5} = 0.0074 + 0.0032V$	Vertical	$A_{0.5} = 0.0337 + 0.0047V$
	$A_{0.75} = 0.0103 + 0.0041V$		$A_{0.75} = 0.0429 + 0.0056V$
	$A_{2\sigma} = 0.0242 + 0.0056V$		$A_{2\sigma} = 0.0741 + 0.0065V$
	$A_{3\sigma} = 0.0870 + 0.0053V$		$A_{3\sigma} = 0.1533 + 0.0059V$

Source(s): Authors' own work

Table 6. Statistic relationship between speed and car body acceleration under different quantiles

5. Conclusion

This study proposed a novel data-driven approach to explore the influence of speed on car body acceleration. Further, technical support was provided for track service status assessment and irregularity control. We developed a low-cost sensing terminal that can be installed on commercial trains. It is a non-invasive acceleration measurement device that need not be powered by operating vehicles, greatly improved the acceleration measurement efficiency, and realized high-frequency measurement of in-service train acceleration that cannot be measured by the TGC. It recorded the car body acceleration during the evolution of the track state as important data support for track departments to assess the track status and formulate maintenance plans.

Data from 272 metro sections measured using eight sensing terminals were used as a case study. The probability distribution of car body acceleration was mainly concentrated to the constant speed stage, particularly when the speed was 15.4, 18.3, and 20.9 m/s. The data balance was realized based on the probability distribution of car body acceleration in different speed ranges. Combined with the traditional linear relationship between the speed and acceleration, the statistical relationships between the speed and car body acceleration within different quantiles were determined. We recommend lateral and vertical τ quantiles of 0.8989 and 0.9895, 0.9942 and 0.997, and 0.9998 and 0.993 regression as excellent, good, and qualified control limits, respectively, for car body lateral and vertical acceleration. In addition, the regression lines for the speed-related acceleration limits at other quantiles (0.5, 0.75, 2σ, and 3σ) were obtained.

Car body acceleration is attributable to the combined effects of the vehicle–track interaction system and several other factors. Because the quantile regression model exhibited strong robustness, the influence of speed on car body acceleration can be considered under the combined actions of multiple factors. Therefore, the proposed method can be used as a basis for formulating an acceleration-limit standard for rail transit.

References

Abdulrazagh, P., Hendry, M., Gül, M., Roghani, A., & Toma, E. (2022). Use of measured accelerations from a passenger rail car to evaluate ride quality and track roughness – a case study. *Proceedings of the Institution of Mechanical Engineers, Part F: Journal of Rail and Rapid Transit*, *236*(6), 733–742. doi: 10.1177/09544097211041459.

Ahlin, K., & Granlund, N. (2002). Relating road roughness and vehicle speeds to human whole-body vibration and exposure limits. *International Journal of Pavement Engineering*, *3*(4), 207–216. doi: 10.1080/10298430210001701.

Audley, M., & Andrews, J. (2013). The effects of tamping on railway track geometry degradation. *Proceedings of the Institution of Mechanical Engineers, Part F: Journal of Rail and Rapid Transit*, *227*(4), 376–391. doi: 10.1177/0954409713480439.

Cong, J., Gao, M., Wang, Y., Chen, R., & Wang, P. (2020). Subway rail transit monitoring by built-in sensor platform of smartphone. *Frontiers of Information Technology & Electronic Engineering*, *21*(8), 1226–1238. doi: 10.1631/fitee.1900242.

Correia, J., Pedrosa, B., Raposo, P., Jesus, A., Gervasio, H., Lesiuk, G., . . . Silva, L. (2017). Fatigue strength evaluation of resin-injected bolted connections using statistical analysis. *Engineering*, *3*(6), 795–805. doi: 10.1016/j.eng.2017.12.001.

Haigermoser, A., Luber, B., Rauh, J., & Graefe, G. (2015). Road and track irregularities: Measurement, assessment, and simulation. *Vehicle System Dynamics*, *53*(7), 878–957. doi: 10.1080/00423114.2015.1037312.

He, Y., Zheng, Y., & Xu, Q. (2019). Forecasting energy consumption in Anhui province of China through two Box-Cox transformation quantile regression probability density methods. *Measurement*, *136*, 579–593. doi: 10.1016/j.measurement.2019.01.008.

Higgins, C., & Liu, X. (2018). Modeling of track geometry degradation and decisions on safety and maintenance: A literature review and possible future research directions. *Proceedings of the Institution of Mechanical Engineers, Part F: Journal of Rail and Rapid Transit*, *232*(5), 1385–1397. doi: 10.1177/0954409717721870.

Hodge, V., O'Keefe, S., Weeks, M., & Moulds, A. (2015). Wireless sensor networks for condition monitoring in the railway industry: A survey. *IEEE Transactions on Intelligent Transportation Systems*, *16*(3), 1088–1106. doi: 10.1109/tits.2014.2366512.

Kim, Y., Kwon, H., Kim, S., Park, C., & Park, T. (2003). Correlation of ride comfort evaluation methods for railway vehicles. *Proceedings of the Institution of Mechanical Engineers, Part F: Journal of Rail and Rapid Transit*, *217*(2), 73–88. doi: 10.1243/095440903765762823.

Kulkarni, R., Qazizadeh, A., Berg, M., Carlsson, U., & Stichel, S. (2022). Vehicle running instability detection algorithm (vrida): A signal based onboard diagnostic method for detecting hunting instability of rail vehicles. *Proceedings of the Institution of Mechanical Engineers, Part F: Journal of Rail and Rapid Transit*, *236*(3), 262–274. doi: 10.1177/09544097211020578.

Lasisi, A., & Attoh-Okine, N. (2018). Principal components analysis and track quality index: A machine learning approach. *Transportation Research Part C: Emerging Technologies*, *91*, 230–248. doi: 10.1016/j.trc.2018.04.001.

Lederman, G., Chen, S., Garrett, J., Kovacevic, J., Noh, H., & Bielak, J. (2017). Track monitoring from the dynamic response of a passing train: A sparse approach. *Mechanical Systems and Signal Processing*, *90*, 141–153. doi: 10.1016/j.ymssp.2016.12.009.

Lee, J., Choi, S., Kim, S., Kim, Y. G., & Park, C. (2012). Waveband analysis of track irregularities in high-speed railway from on-board acceleration measurement. *Journal of Solid Mechanics and Materials Engineering*, *6*(6), 750–759. doi: 10.1299/jmmp.6.750.

Li, C., He, Q., & Wang, P. (2022). Estimation of railway track longitudinal irregularity using vehicle response with information compression and Bayesian deep learning. *Computer-aided Civil and Infrastructure Engineering*, *37*(10), 1260–1276. doi: 10.1111/mice.12802.

Mohammadi, R., He, Q., Ghofrani, F., Pathak, A., & Aref, A. (2019). Exploring the impact of foot-by-foot track geometry on the occurrence of rail defects. *Transportation Research Part C: Emerging Technologies*, *102*, 153–172. doi: 10.1016/j.trc.2019.03.004.

Mori, H., Sato, Y., Ohno, H., Tsunashima, H., & Saito, Y. (2013). Development of compact size onboard device for condition monitoring of railway tracks. *Journal of Mechanical Systems for Transportation and Logistics*, *6*(2), 142–149. doi: 10.1299/jmtl.6.142.

Shan, Y., Wang, B., Zhang, J., & Zhou, S. (2021). The influence of dynamic loading and thermal conditions on tram track slab damage resulting from subgrade differential settlement. *Engineering Failure Analysis*, *128*, 105610. doi: 10.1016/j.engfailanal.2021.105610.

Shan, Y., Li, X., & Zhou, S. (2023). Multi-objective optimisation methodology for stiffness combination design of bridge-embankment transition zones in high-speed railways. *Computers and Geotechnics*, *155*, 105242. doi: 10.1016/j.compgeo.2022.105242.

Sun, J., Chi, M., Cai, W., Gao, H., & Liang, S. (2021). An investigation into evaluation methods for ride comfort of railway vehicles in the case of carbody hunting instability. *Proceedings of the Institution of Mechanical Engineers, Part F: Journal of Rail and Rapid Transit*, *235*(5), 586–597. doi: 10.1177/0954409720949116.

Tsunashima, H., & Hirose, R. (2020). Condition monitoring of railway track from car-body vibration using time-frequency analysis. *Vehicle System Dynamics*, *60*(4), 1170–1187. doi: 10.1080/00423114.2020.1850808.

Tsunashima, H., Naganuma, Y., & Kobayashi, T. (2014). Track geometry estimation from car-body vibration. *Vehicle System Dynamics*, *52*(1), 207–219. doi: 10.1080/00423114.2014.889836.

UIC 515-1 (n.d.). Passenger rolling stock - trailer bogies - running gear - general provisions applicable to the components of trailers bogies.

Wang, Y., Cong, J., Wang, P., Liu, X., & Tang, H. (2019). A data-fusion approach for speed estimation and location calibration of a metro train based on low-cost sensors in smartphones. *IEEE Sensors Journal*, *19*(22), 10744–10752. doi: 10.1109/jsen.2019.2933638.

Wei, X., Liu, F., & Jia, L. (2016). Urban rail track condition monitoring based on in-service vehicle acceleration measurements. *Measurement*, *80*, 217–228. doi: 10.1016/j.measurement.2015.11.033.

Xu, L., & Zhai, W. (2017a). A new model for temporal–spatial stochastic analysis of vehicle–track coupled systems. *Vehicle System Dynamics*, *55*(3), 427–448. doi: 10.1080/00423114.2016.1270456.

Xu, L., & Zhai, W. (2017b). A novel model for determining the amplitude-wavelength limits of track irregularities accompanied by a reliability assessment in railway vehicle-track dynamics. *Mechanical Systems and Signal Processing*, *86*, 260–277. doi: 10.1016/j.ymssp.2016.10.010.

Xu, L., & Zhai, W. (2018). Probabilistic assessment of railway vehicle-curved track systems considering track random irregularities. *Vehicle System Dynamics*, *1*(10), 1–25. doi: 10.1080/00423114.2018.1424916.

Yu, K., Lu, Z., & Stander, J. (2003). Quantile regression: Applications and current research areas. *Journal of the Royal Statistical Society: Series D-(The Statistician)*, *52*(3), 331–350. doi: 10.1111/1467-9884.00363.

Zoccali, P., Loprencipe, G., & Lupascu, R. (2018). Acceleration measurements inside vehicles: Passengers' comfort mapping on railways. *Measurement*, *129*, 489–498. doi: 10.1016/j.measurement.2018.07.079.

Further reading

Technical Specification for Interoperability (TSI) (n.d.). 'Rolling Stock — locomotives and passenger rolling stock' subsystem of the rail system in the European Union issued on 18 November 2014.

Torstensson, P., & Nielsen, J. (2011). Simulation of dynamic vehicle–track interaction on small radius curves. *Vehicle System Dynamics*, *49*(11), 1711–1732. doi: 10.1080/00423114.2010.499468.

Corresponding author

Zilong Wei can be contacted at: weizl1988@163.com